Influence of an absorbers GEM_{PEHD} thermal properties on the propagation of heat in a solar sensor

BABA AHMED Nassim[1], ALIANE Khaled[1], BENMOUSSAT Abderrahim[2]
1Department of Physique, Faculty of Science, Abou Bekr Belkaïd University of Tlemcen, Tlemcen, Algeria
2Materials sciences and Environment Group, Faculty of sciences and Technology, Department of matter sciences, Tamanrasset University center, BP 10034 SERSOUF, Tamanrasset - ALGERIA

Abstract. This paper presents an experimental study to measure some physic-chemical properties of a high-density polyethylene geomembrane (GEM_{PEHD}) in a temperature range from 300 K to 400 K. The results will yield a dependency between temperature and its properties in order to study an energy and process the thermal aging GEM_{PEHD} on the solar collector. In the energy study, we solve the nonlinear equation of unsteady heat with as main non linearity influence of different properties GEM_{PEHD} on the solar collector and one notes that the GEM_{PEHD} presented a maximum exchange Thermal characterized by high absorption and low reflection. Thus, increasing the power absorbed by the GEM_{PEHD} increases its temperature and the useful power received by the air and then the air temperature. Overall losses increase with the increase of the temperature difference between the GEM_{PEHD} and windows and this increases the efficiency of the solar collector and minimize the entropy of the system. Then the study of thermal aging is dedicated to the interpretation of various analyses on GEM_{PEHD} before and after its use in the solar collector. The thermal aging GEM_{PEHD} in the air is a physical loss and chemical consumption immediately followed by a brutal oxidation of the polymer. The losses would be governed primarily by the chemical consumption of antioxidants. After various tests, we conclude that the value of using the GEM_{PEHD} as absorber in the solar collector is doubly beneficial. First, given its very attractive cost compared to other as efficient absorbers (such as metals) gives good thermal performance of the solar collector even reaching 72%. While the life of the GEM_{PEHD} is rather long (several years).

1. Introduction:

Interest in solar air heating has resulted in recent years by the appearance on the market of a number of systems, which include solar collectors. The motivation of this work focuses on the following findings: An environmental statement to limit the intensity of the greenhouse effect and rising temperatures on the surface of the planet by which action plans for emission limitation some greenhouse gases (GHG) have been implemented by many countries. An energy finding where energy needs are growing throughout the four corners of the planet. The industrial sector **[1]** remains the main consumer of energy and the residential and commercial sectors consume mainly because of space heating and coins. The production and consumption of energy contribute to the change in thermal equilibrium at the surface of the earth by producing greenhouse gases that are assigned the current warming of the planet. At that thermal pollution also complemented by a physical or chemical waste pollution **[2]**.

One of problems in solar capture is the choice of materials and their selectivity to optimize absorption and reduce heat transfer through the insulation or transparent materials to reduce reflections and get the maximum radiation converts. We are interested in this study to the polymer material, the high-density polyethylene geomembrane (GEM_{PEHD}) used as a heat absorber in the solar collector energy study that will form during sun exposure. Then, we study the influence of aging on the sustainability and efficiency of the solar collector.

2. Materials and methods:

We use various experimental techniques for physicochemical characterization as well as aging of the samples GEM_{PEHD} to assess the structural and textural properties of our material. In addition, we will present numerical method for modelling the nonlinear equation of unsteady heat. The GEM_{PEHD}, used in this study, is a polymer that provide to us as granules stabilized with antioxidants and process the nature of which has not been

specified us. This polymer corresponds to the basic matrix of a commercial GEM. The PE100: it is a PEHD was added 0.4% by weight of a phenolic antioxidant, Irganox B225. Our material has endured aging accelerates high temperature in a ventilated oven in air at atmospheric pressure in order to follow the structural evolution during the period of exposure in the solar sensor.

- Emissivity: The method allows the measurement of the hemispherical directional reflectivity and there after calculate the emissivity of the surface using a portable emissometer **[3, 4, and 5]**. The current equipment design for easy use in the field and better to control of the operation of the infrared source; it allows achieving emissivity measurements in different wavelength bands that the optical detector can be replaced very easily. The method chosen for the characterization of the density is that of the pycnometer. The measurements made with a pycnometer to a balance and small amounts (1 to 4 g) for GEM_{PEHD}. The pycnometer used has a marked capillary to measure a precise volume.
- Thermal Conductivity and Thermal diffusivity: We propose a measuring method enabling the simultaneous characterization of the thermal conductivity (k) and thermal diffusivity (a) a sample of the GEM_{PEHD} at room temperature **[6]**. We modulate the temperature of the sample and measure the temperature variations on each of its faces. The measurements performed under vacuum (pressure < 10^{-4} mbar) to reduce convection losses on the sides.
- ATG thermal analysis of samples conducted used is of type SDT Q600. The analysis performed in air with a temperature ramp of 5 ° C / min in the range of 25 to 1200 ° C for a few samples at 1000 ° C for others.
- UV-visible diffuse reflection analysis and differential scanning calorimetry performed on a Perkin Elmer Lambda 800 flown from a microcomputer.
- Infrared analysis in Fourier transform (FTIR) was performed using an Avatar 320 FT-IR spectrometer THERMO-NICOLET. Spectra were recorded either transmittance (T) or absorbance (A) between 4000 cm^{-1} and 400 cm^{-1}. The X-ray diffraction (DRX) performed with a PANalytical X'Pert diffractometer type Pro goniometer with a theta / theta.
- Solar sensor: The test bench was performed at the University of Tlemcen lying north-west Algeria at latitude 35.28 degrees, a longitude of -1.17° and an altitude of 750 m. It is characterized by lots of sunshine, with an average daily irradiation 6000Wh / m², a sunshine duration of 3000 hours a year and a clearness index K_t average of 0.75 **[7]**. The solar sensor is shown in **Figure 1**, the total area of 2.6 m², and the opening area equal to 2.4 m². It is mounted on a rigid adjustable steel structure with a 45° inclination.

The solar sensor is a parallelepiped shape, constructed with galvanized sheet metal (thickness e = 1.5 mm, length L = 1 m, width = 0.2 m and the thickness of the air gap H = 1 cm). It is internally reinforced by angle irons, covered outside by wooden cork as a thermal insulator between the two there is a glass wool layer of 5 cm thickness on the side surfaces and on the rear surface. Inside the metal sheet is covered by 5 mm thickness GEM_{PEHD} as a heat absorber. Two panes of 4 mm thick form the transparent cover each with a space between two panes of 1.5 cm as recommended in the literature **[8]** because this minimizes the edge effect while maintaining low loss by convection. In this study, we are interested in the front part of the solar collector, the heat from the solar rays that pass through the glass and is absorbed by the inner face of the wall placed on the absorber. The lower face is subjected to a constant heat flux simulating the energy received by the solar radiation on a face of negligible thickness.

Figure 1: Solar collector

3. Results and discussion:

We recap some intrinsic properties of the GEM_{PEHD} in **Table 2**. **Table 2:** Intrinsic properties of the GEM_{PEHD}

Properties	Unit	Value
Volumes' density	$g.cm^{-3}$	0,974 ± 0,01
Thermal conductivity	$W/m \cdot K$	0,28 ± 0,01
Thermal diffusivity	m^2/s	$(0{,}314 \pm 0{,}02) \cdot 10^{-6}$
Density*	g/cm	0,949 ± 0,001
Temperature of fusion**	°C	135,7 ± 0,1
Degree of crystallinity**	%	78 ± 2
Weight average molar mass***	g / mol	500,4 ± 0,4
Glass transition temperature	°C	- 125
Coefficient of expansion	C^{-1}	$19 \cdot 10^{-5}$

* Measured by a weighing device on a Mettler TOLEDO in air and in acetone.
** Measured by differential scanning calorimetry with a temperature rise rate of 10 ° C.min-1 in an inert atmosphere.
*** Measured by steric exclusion chromatography at 145 ° C in 1,2,4 trichlorobenzene with a chromatographic system equipped with a triple detection (Viscometer, refractive index and Laser).

The value of the specific heat capacity of the GEM_{PEHD} given by calculating the value of C_p from the values of measured density, conductivity and thermal diffusivity using the following relationship

$$C_P = \frac{k}{a \cdot \rho} \qquad (5)$$

The value of the following specific heat capacity is $(2300 \pm 0{,}012)\ \ J/Kg \cdot K$.

Spectral emissivity remains measured at room temperature, approximately 20 °C. The results illustrated in **Figure 2**. This figure shows that the emissivity varies little within this range of temperatures and wavelengths.

Figure 3 shows that the emissivity of the GEM_{PEHD} reaches a constant value for a sample of thickness greater than 0.2 mm. We find the value 0.93 determined above. Beyond this thickness, GEM_{PEHD} may considered opaque with respect to the IR radiation.

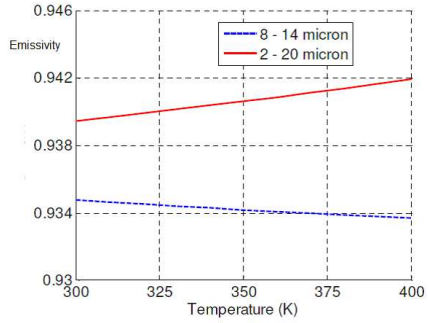

Figure 2: Emissivity of GEM_{PEHD}

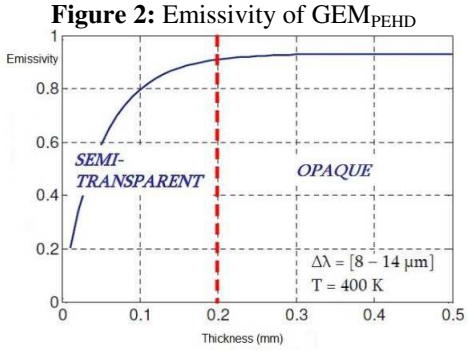

Figure 3: Total Emissivity of GEM_{PEHD}

3.1. *Energy study on the solar collector*: The **figure 4** gives us the intensity of the solar flux for the four days that are respectively 17 January, 15 May, 16 August and 15 October 2015. It noted that the intensity of the solar flux is greater in the days of May 15 and August 16 in which the days are longer.

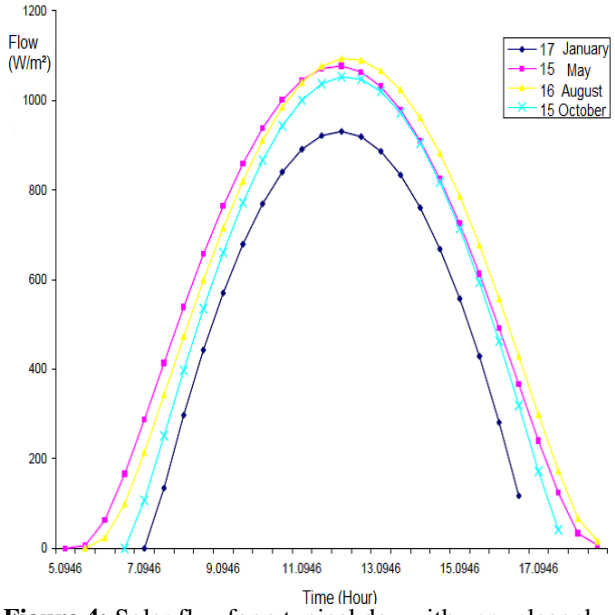

Figure 4: Solar flux for a typical day with very clear sky

To see the effect of climatic parameters on changes in air temperature T_F, weather data was used (direct radiation, wind speed and ambient temperature) measured by the meteorological station in Tlemcen site for day of 16 August 2015. We introduced the values measured in the simulating program of the T_F area, to see the differences compared to the values obtained by semi-empirical models. These data shown in **Figures 5 and 6**. It noted that the numerically values obtained are close to those of the experimental data, the effect of wind speed and room temperature is almost negligible.

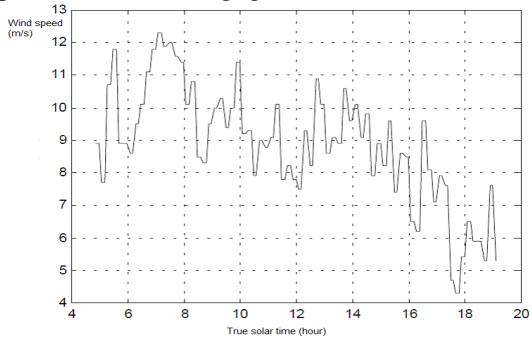

Figure 5: Experimental measurements of wind speed for 16 August 2015

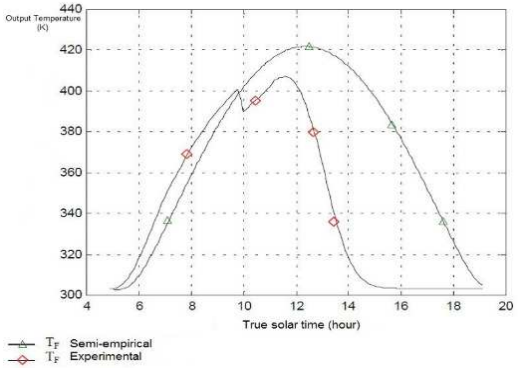

Figure 6: Simulation of the outlet air temperature for 16 August 2015

In the range of airflow values studied from 20 to 200 kg/h, **figure 7** shows the experimental values from previous work **[11]** and are very close to this configuration, in order to validate our approach digital. We note that the experimental values of the instantaneous thermal efficiency of the solar collector is not very far from the values from the theoretical models. However, for low flows, the model overestimates the performance. We believe that this discrepancy can explained on one hand by measurement errors but mostly by theoretical approaches made at the equated the theoretical model are the underestimation of losses in the theoretical model amounted for low airflow rates, because of the higher temperature difference between the absorber and the outside. We could introduce empirical correction coefficient of overall losses, from experimental data, as was done in **[12]**. In this work, the evolution of the overall losses U_L coefficient was plotted against the temperature difference $(T_f - T_a)$ which is all the more important that the flow rate is low, T_f being the average air temperature within the air gap and the ambient temperature T_a. The proposed equation is of the form $U_L = a\ (T_f - T_a)^b$. The evolution of the instantaneous thermal

efficiency of the solar collector shown in **Figure 8**. We note that the addition of GEM_{PEHD} absorber made a remarkable increase is about 25% relative to a solar collector with another type absorber. Analysis of the various results obtained show that while the duration of the capture of solar radiation near room temperature, the solar collector has a good performance, which is around 55%. This performance explained by lower optical and thermal losses through the glazing system. Taking into account the means of realization of our system, its simplicity and its cost price is quite low and compared to other more sophisticated solar collector performance found in the literature, we can conclude that our prototype still competitive with a quality / price very valuable. Based on experimental tests on our system and the different results obtained, we find that more solar illumination is perpendicular to the greater the amount of heat absorbed collecting area is considerable, because the glazing transitivity and absorptivity of the absorbing plate are inversely proportional to the angle of incidence of solar radiation. It is therefore very important to choose the inclination of the solar collector with the seasons to take better advantage of the system.

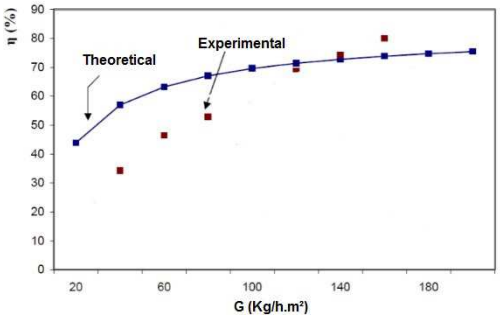

Figure 7: Thermal efficiency of the solar collector as a function of airflow

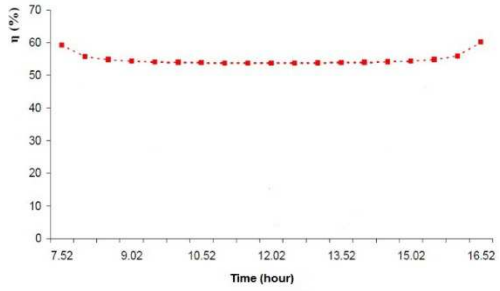

Figure 8: Change thermal efficiency of the solar collector with a clear sky and a throughput of 35 kg / h.

As regards the development of in and out air temperatures, the results confronted with experimentally provides those delivered digitally. **Figure 9** shows the temporal variation of the temperature of each sensor element. In this figure, the absorber and the inner surface of the insulator have higher temperatures, this is due to the power absorbed by the absorber is important and is greater than that absorbed by the glass, and the insulation is placed beneath the absorber plate, the latter has a high thermal conductivity. The lowest temperature is that of the insulation of the rear side, indicating that the insulation has low thermal conductivity. The increase in indoor and outdoor temperatures glazing is due to absorption by the window of the incident solar radiation and the heat released by the absorber. The temperature of the inner surface is slightly greater than that of the outer face; this is due to the trapping of solar infrared ray inside the sensor thereby increasing the temperature inside of the glass with respect to outside, which assigned to the action of wind. The coolant outlet temperature is slightly lower than that of the absorber, due to losses. The analysis results successively shows good agreement between the results provided by the model and those found in the literature. It is reported that due to the existing deviations from the experimental and theoretical work cited, compared with those of our modeling, are due to the aging phenomenon of the constituent elements the solar collector when it comes to enter the corresponding values thermophysical and optical parameters, on the other hand the illuminations seem unfitted models considered under specific conditions.

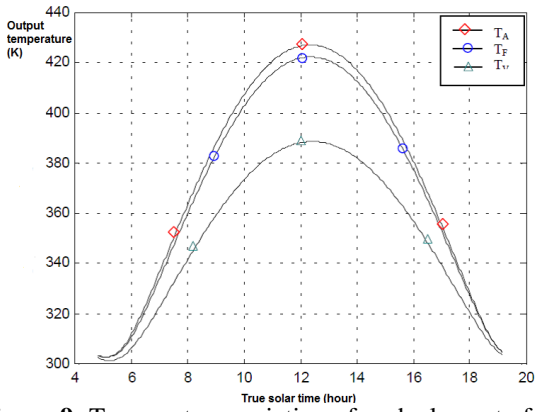

Figure 9: Temperature variation of each element of the sensor

3.2. *Study of aging* GEM_{PEHD}: The samples were prepared after summers spent summers in the solar collector. Each of these techniques giving us access to the results of different origins (chemical, physical), the confrontation of all these data allow us to envisage a better interpretation of the results. Infrared spectroscopy is the first additional technique that we used. A test campaign showed different behavior during the first hours of irradiation. This difference is a greater amount of carbonyls present in the samples prior to irradiation and for other campaigns. The amount of vinyl product remains the same as for other campaigns, and has a similar evolution during irradiation, with two separate steps before and after 6 h of irradiation (**Figure 10**).

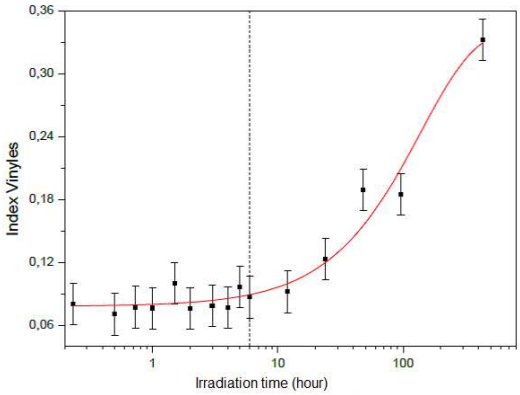

Figure 10: Evolution of vinyl degradation products as a function of UV irradiation time.

The reason for the presence of strong carbonyl degradation product in samples prior to irradiation from the manufacturing protocol. Shaping done on a hot plate at a temperature of 150 °C, to which the GEM_{PEHD} undergoes a major thermal oxidation, which causes formation of carbonyl-type degradation products if the exposure time is too long. We chose to keep this trial campaign since the first moments of exposure to UV show interesting behavior (**Figure 11**) **[13]**.

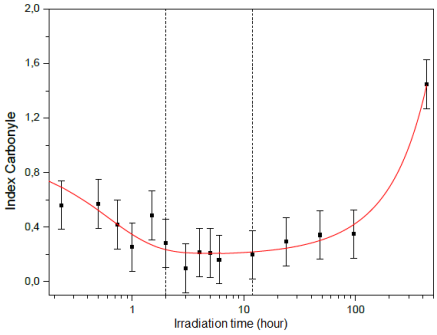

Figure 11: Evolution of carbonyl degradation products as a function of UV irradiation time.

The differential scanning calorimeter used in the following part will allow us to have access to this information. This technique allows us to obtain information on physical samples and especially the degree of crystallinity (% Cr) and the melting temperature (T_f). **Figure 12** shows the change in the rate of crystallinity of the samples according to the UV ray exposure time. As in the case of the infrared spectroscopy analysis, two distinct phases can observed. Crystallinity rate remains stable at around 72% during the first 6 hours, then increases exponentially in the semi logarithmic representation to reach the value of 79% after 18 days of irradiation.

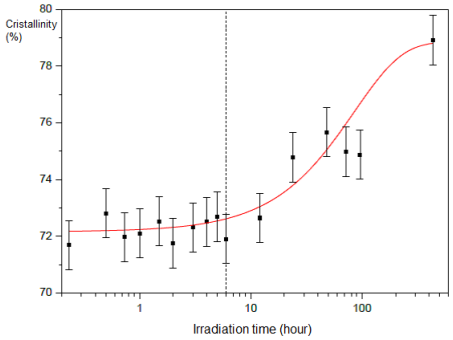

Figure 12: Evolution of crystallinity during the UV irradiation.

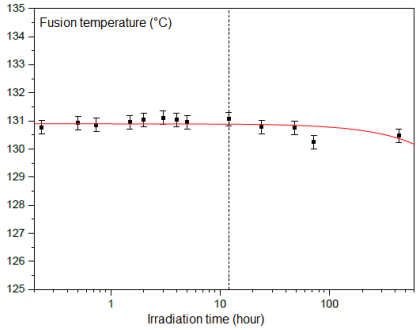

Figure 13: Evolution of the melting temperature of the samples as a function of UV irradiation.

This increase in the degree of crystallinity accompanied by a slight decrease in the melting temperature (**Figure 13**). In the literature, different authors interpret these results by changing the macromolecular chains of GEM_{PEHD} due to UV irradiation. UV radiation causes breaks chains with consequent increases in crystallinity **[14]**. Indeed, in the amorphous phase, chains see their length reduced, making them more mobile **[15]** and thus favoring the phenomenon called secondary crystallization **[16]**, illustrated here by increasing the degree of crystallinity after 6 h of exhibition.

From the melting temperature values and crystallinity, it is possible to calculate the size of the crystal lamellae. Preliminary calculations performed on irradiated samples led to size strips of the order of 30.1 nm. The evolution of this value during the deterioration (**Figure 14**) may also presented in two stages, in the first moments with a stability followed by a decrease. This development is in line with the first results of degree of crystallinity and melting temperature. The rupture of the macromolecular chains caused by UV radiation leading to lamellae smaller dimensions which plays on the melting temperature and the crystallinity. However, even if all the results obtained in AED are well in line with the already established models.

Monitoring of weight average molecular weight of the GEM_{PEHD} during UV irradiation performed by GPC and shows a rapid increase them from an hour of exposure (**Figure 15**). These results are consistent with an increase in the average length of the macromolecular chains, which can attributed to cross-linking phenomena.

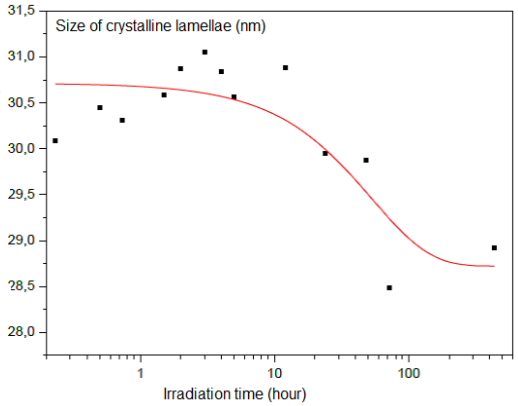

Figure 14: Evolution of the size of crystalline lamellae as a function of UV irradiation time.

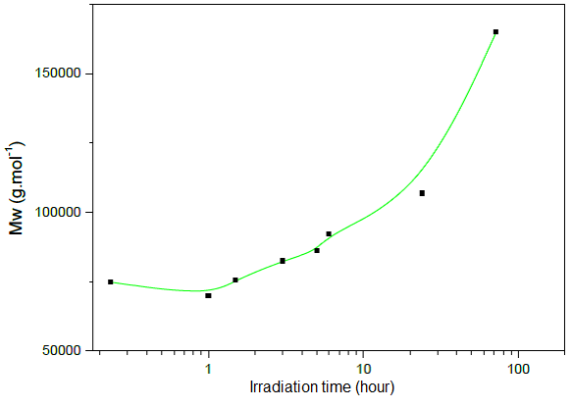

Figure 15: Changes in the average molar mass by weight of the GEM_{PEHD} as a function of UV irradiation time.

4. Conclusion:

The results obtained show that the outlet temperature varies depending on the solar flux as well as geometric and climatic parameters. Among the main results, we quote:

- Large temperature value achieved in the summer solstice, which can reach 420 K in true solar noon. It mainly depends on the power consumption that is a function of the optical and geometrical parameters of the sensor. What say we leave this type of collector can favorably recommended in the water-heating sector.
- The temperature of the absorber is closest to T_F, which can be justified by its high absorptivity for visible solar radiation and a high emissivity for the infrared radiation of long wavelength with its coating. It is possible to keep the greater part of the incident solar energy and not lose as little heat by long wavelength radiation when the absorbent surface becomes hot. The glazing temperature is lower than that of TF when dependent optical, climatic, and specific parameters of the wind speed.

Analyzes performed by FTIR and DSC provide information about aging GEM_{PEHD}. It is found that thermal aging has an important influence on the volumetric strain due to increased crystallinity. The X-ray diffraction analysis showed the post crystallization phenomenon by revelation of the increased crystallinity of the aged sample. While FTIR analysis has shown that, this phenomenon is due only to the change in the structural morphology of the GEM_{PEHD}. Investigations conducted by DSC shows that the GEM_{PEHD} has a melting temperature of 131 °C for an aged sample while valley 135 °C for a blank sample characteristic of increasing the crystallinity of confirming the findings with the same further analyzes.

Each analysis technique having its own sensitivity to this or that phenomenon, aggregation and correlation of all results obtained are essential for a comprehensive understanding of degradation mechanisms GEM_{PEHD}. However, a question remains open on the choice of the molecule inserted into the GEM_{PEHD}, this choice that can condition the type of information obtained. In our case, with Irganox B225, the results show a high sensitivity to rearrangements of the macromolecular chains of the GEM_{PEHD}.

After various tests, we conclude that the value of using the GEM_{PEHD} as absorber in the solar collector is doubly beneficial. First, given its very attractive cost compared to other as efficient absorbers (such as metals) gives good thermal performance of the solar collector even reaching 72%. While the life of the GEM_{PEHD} is rather long (several years).

Reference:

[1] OCDE. Énergie : les cinquante prochaines années. OECD Publishing, 2010.

[2] A. Bidart and L. Dubois, Les énergies fossiles et renouvelables, Dossier Pédagogique de la Fondation Polaire Internationale, 2003.

[3] L. Ibos, S. Datcu and S. Matteï, Mesure d'émissivité totale à température ambiante de matériaux inhomogènes à l'aide d'un émissomètre portable, 5ème Colloque Interuniversitaire Franco-Québécois Thermique des Systèmes, Lyon, 73-80, 2001.

[4] L. Ibos, M. Marchetti, A. Boudenne, S. Datcu, J. Livet and Y. Candau, Infrared emissivity measurement device : Principle and applications, Measurement Science and Technology, 17, 2950-2956, 2006.

[5] M. Marchetti, L. Ibos, A. Boudenne, S. Datcu, Y. Candau, J. Dumoulin and J. Livet, Analyse du comportement radiatif de matériaux de l'infrastructure routière : Principes et mesures de l'émissivité infrarouge, Bulletin des Laboratoires des Ponts et Chaussées, 272, 45-55, 2008.

[6] E. Tang-Kwor, Contribution au développement de méthodes périodiques de mesure de propriétés thermophysiques des matériaux opaques, Thèse Université Paris 12, 1998.

[7] Ministère de l'Energie et des Mines, Bilan énergétique nationale de l'année 2010, www.mem-algeria.org, 2011.

[8] N. M. Nahar and P. G. Jagdish, Studies on gap spacing between absorber and cover glazing in flat plate solar collectors, International journal of energy research, 13, 1989.

[9] S. W. Churchill and H. S. Chu, Correlating Equations for Laminar and Turbulent Free Convection from a Vertical Plate, *International Journal of Heat and Mass Transfer,* 18, 1323-1329, 1975.

[10] B. Cheron, *Transferts Thermiques - Résumé De Cours, Problèmes Corrigés*, Ellipses marketing, 1999.

[11] I. Tari, Natural convection simulations and numerical determination of critical tilt angles for a parallel plate channel, Energy conversion and management, 51, 685-695, 2010.

[12] R. Alvarado, J. Xamán, J. Hinojosa and G. Álvarez, Interaction between natural convection and surface thermal radiation in tilted slender cavities, International Journal of thermal sciences, 47, 355–368, 2008.

[13] Q. Wu and al., *Surface photo-oxidation and photostabilization of photocross-linked olyethylene,* Polymer Degradation and Stability, 68(1), 97-102, 2000.

[14] R. Yang and al., *Effects of inorganic fillers on the natural photo-oxidation of high-density Polyethylene,* Polymer Degradation and Stability, 88(2), 333-340, 2005.

[15] L. Guadagno and al., *Chemical and morphologial modifications of irradiated linear low density polyethylene,* Polymer Degradation and Stability, 72(1), 175-186, 2001.

[16] I. H. Craig and al., *Photo-induced scission and crosslinking in PELD, PELLD and PEHD,* Polymer Engineering and Science, 45(4), 579-587, 2005.